

High-power Femtosecond Optical Parametric Amplification at 1 kHz in BiB₃O₆ pumped at 800 nm

Valentin Petrov, Frank Noack and Pancho Tzankov

Max-Born-Institute for Nonlinear Optics and Ultrafast Spectroscopy, 2A Max-Born-Str. D-12489 Berlin, Germany
petrov@mbi-berlin.de

Masood Ghotbi and Majid Ebrahim-Zadeh

ICFO-The Institute of Photonic Sciences, Mediterranean Technology Park, E-08860 Castelldefels, Barcelona, Spain

Ivailo Nikolov and Ivan Buchvarov

Faculty of Physics, Sofia University, 5 James Bourchier Blvd., BG-1164 Sofia, Bulgaria

Abstract: Substantial power scaling of a travelling-wave femtosecond optical parametric amplifier, pumped near 800 nm by a 1 kHz Ti:sapphire laser amplifier, is demonstrated using monoclinic BiB₃O₆ in a two stage scheme with continuum seeding. Total energy output (signal plus idler) exceeding 1 mJ is achieved, corresponding to an intrinsic conversion efficiency of ≈32% for the second stage. The tunability extends from 1.1 to 2.9 μm. The high parametric gain and broad amplification bandwidth of this crystal allowed the maintenance of the pump pulse duration, leading to pulse lengths less than 140 fs, both for the signal and idler pulses, even at such high output levels.

©2007 Optical Society of America

OCIS codes: (190.4970) Parametric oscillators and amplifiers; (190.4400) Nonlinear optics, materials; (190.7110) Ultrafast nonlinear optics.

References and links

1. F. Seifert, V. Petrov, and F. Noack, "Sub-100-fs optical parametric generator pumped by a high-repetition-rate Ti:sapphire regenerative amplifier system," *Opt. Lett.* **19**, 837-839 (1994).
2. V. Petrov, F. Seifert, and F. Noack, "High repetition rate traveling wave optical parametric generator producing nearly bandwidth limited 50 fs infrared light pulses," *Appl. Phys. Lett.* **65**, 268-270 (1994).
3. G. Cerullo, S De Silvestri, M. Nisoli, S. Sartania, S. Stagira, and O. Svelto, "Few-optical-cycle laser pulses: From high peak power to frequency tunability," *IEEE J. Sel. Top. Quantum. Electron.* **6**, 948-958 (2000).
4. G. Cerullo and S. De Silvestri, "Ultrafast optical parametric amplifiers," *Rev. Sci. Instrum.* **74**, 1-18 (2003).
5. V. Petrov, F. Rotermund, and F. Noack, "Generation of high-power femtosecond light pulses at 1 kHz in the mid-infrared spectral range between 3 and 12 μm by second-order nonlinear processes in optical crystals," *J. Opt. A: Pure Appl. Opt.* **3**, R1-R19 (2001).
6. M. Nisoli, S. De Silvestri, V. Magni, O. Svelto, R. Danielius, A. Piskarskas, G. Valiulis, and A. Varanavicius, "Highly efficient parametric conversion of femtosecond Ti:sapphire laser pulses at 1 kHz," *Opt. Lett.* **19**, 1973-1975 (1994).
7. K. R. Wilson and V. V. Yakovlev, "Ultrafast rainbow: tunable ultrashort pulses from a solid-state kilohertz system," *J. Opt. Soc. Am. B* **14**, 444-448 (1997).
8. R. Danielius, A. Piskarskas, A. Persson, and S. Svanberg, "Widely tunable β-BaB₂O₄ parametric laser pumped by femtosecond Ti:sapphire laser-amplifier system," *Lithuanian Phys. Journal* **33**, 245-248 (1993).
9. H. Hellwig, J. Liebertz, and L. Bohaty, "Exceptional large nonlinear optical coefficients in the monoclinic bismuth borate BiB₃O₆ (BIBO)," *Sol. State Commun.* **109**, 249-251 (1999).
10. H. Hellwig, J. Liebertz, and L. Bohaty, "Linear optical properties of the monoclinic bismuth borate BiB₃O₆," *J. Appl. Phys.* **88**, 240-244 (2000).
11. M. Ghotbi, A. Esteban-Martin, and M. Ebrahim-Zadeh, "Optical parametric generation and amplification in BiB₃O₆," Conference on Lasers and Electro-Optics CLEO 2006, OSA Technical Digest CD-ROM (OSA, Washington, DC 2006), paper JThC64.

12. M. Ghotbi, M. Ebrahim-Zadeh, V. Petrov, P. Tzankov, and F. Noack, "Efficient 1kHz femtosecond optical parametric amplification in BiB₃O₆ pumped at 800 nm," *Opt. Exp.* **14**, 10621-10626 (2006).
13. P. Tzankov and O. Steinkellner, "High-energy Ti:sapphire laser system at 1 kHz optimised for efficient frequency conversion," Conference on Lasers and Electro-Optics, CLEO/Europe-EQEC'05, Munich, Germany, June 12-17, 2005, paper CA8-1-TUE, CLEO/Europe-EQEC 2005 Conference Digest CD-ROM.
14. R. Danielius, A. Piskarskas, A. Stabinis, G. P. Banfi, P. Di Trapani, and R. Righini, "Traveling-wave parametric generation of widely tunable, highly coherent femtosecond light pulses," *J. Opt. Soc. Am.* **10**, 2222-2232 (1993).
15. P. Tzankov and V. Petrov, "Effective second-order nonlinearity in acentric optical crystals with low symmetry," *Appl. Opt.* **44**, 6971-6985 (2005).
16. B. Bareika, A. Birmontas, G. Dikchys, A. Piskarskas, V. Sirutkaitis, and A. Stabinis, "Parametric generation of picosecond continuum in near-infrared and visible ranges on the basis of a quadratic nonlinearity," *Sov. J. Quantum Electron.* **12**, 1654-1656 (1982) [transl. from *Kvantovaya Elektron.* (Moscow) **9**, 2534-2536 (1982)].

The first high-energy femtosecond optical parametric generators and amplifiers (OPGs and OPAs) of the travelling-wave type, pumped by amplified Ti:sapphire laser systems operating near 800 nm at 1 kHz repetition rate, were demonstrated in the early 1990's [1, 2]. This was possible not only due to the fact that such reliable and stable pump sources had just become available but also due to the almost simultaneous introduction of the nonlinear crystals β -BaB₂O₄ (BBO) and LiB₃O₅ (LBO). Today such devices, based primarily on type-II interaction in BBO, are widely available commercially and serve also as the basis for further frequency conversion into the UV and mid-IR. Their broad tunability and flexibility has in fact had an important impact on the development of Ti:sapphire regenerative amplifiers for which the tunability is no longer regarded as an important feature. The further development of such high-power parametric devices for down-conversion has been focused mainly on the achievement of ultimately short pulse durations in the visible and near-IR by utilizing noncollinear geometry, pumping with the second harmonic blue pulses, and seeding with white light continuum (WLC) generated by a single filament in sapphire [3, 4], or the use of non-borate crystals for direct extension into the mid-IR [5]. Little attention, however, has been paid to higher energy scaling. In fact, the highest output energy (signal plus idler) reported at 1-kHz was about 150 μ J for a signal wavelength near 1250 nm (3 stages of BBO type-II OPG and OPA) which corresponds to a total conversion efficiency of 30% for the last stage and 20% for the entire set-up [6]. Such conversion efficiencies are considered to be maximum or optimum before deterioration of the pulse quality, caused by back-conversion processes, occurs. Although conversion efficiencies as high as 45% for the final stage have also been reported, no information on the temporal and spectral quality of the signal and idler pulses was provided in this case [7].

Scaling to much higher energies has been already demonstrated with BBO at low (10 Hz) repetition rate (i.e. at low average powers) and a maximum overall efficiency of 20% was achieved near degeneracy for 10 mJ pump pulses at 795 nm [8]. However, the pulse-to-pulse fluctuations are much stronger at such repetition rates and for many applications it is desirable to have high output energy at kHz repetition rates. In this work we investigate large aperture bismuth triborate, BiB₃O₆ (BIBO), crystals for energy scaling of a high power WLC seeded OPA in the 1.1-2.9 μ m spectral range, pumped at 1 kHz by the fundamental of a specially designed regenerative/multipass Ti:sapphire amplifier. In addition we study the compressibility of the signal pulses in the 1.2-1.4 μ m spectral range.

BIBO is an interesting and relatively new nonlinear optical crystal belonging to the borate family. Its main advantage is the exceptionally high second order nonlinear susceptibility [9]. The effective nonlinearity d_{eff} of BIBO can be larger than that of KTP and the lower transparency edge extends deeper into the UV (286 nm) [10]. These characteristics make this material ideal for down-conversion of amplified femtosecond pulses from the 800 nm region because two-photon absorption should be absent. OPG/OPA operation of BIBO was demonstrated previously only at 10 Hz, using 35 ps long pump pulses at 532 nm [11]. More recently we implemented BIBO in a conventional low-power femtosecond OPA pumped at

800 nm and obtained an output of 80 μJ (signal plus idler) at 1 kHz repetition rate [12]. Here we report energy scaling to above 1 mJ at the same repetition rate.

The experimental set-up used in the present work is shown in Fig. 1. The OPA is pumped by a home-made Ti:sapphire amplifier system which provides pulses of 135 fs duration (Gaussian shape assumption) with an energy of up to 12 mJ [13]. For the present experiment a maximum pump energy of 5 mJ (average power of 5 W) was used, limited by the available aperture of the nonlinear crystals. The central wavelength of the pump pulses was about 807 nm and their spectral width corresponded to a time-bandwidth product of 0.62.

Several μJ of pump energy were focused onto a 2-mm thick sapphire plate to generate a single filament WLC (Fig. 1). The Stokes spectral portion of the WLC pulse was used to seed the first OPA stage at the signal wavelength. In the first stage we employed a 3-mm thick uncoated BIBO crystal with an aperture of $7\times 7\text{ mm}^2$. This crystal was cut at $\theta=42^\circ$ in the x-z principal plane ($\varphi=0^\circ$), for $o\rightarrow eo$ interaction. As in the case of BBO [4], the advantages of using type-II interaction are related to the possibility to tune, even close to degeneracy, at almost constant bandwidth for the signal and idler. Similar to type-II BBO, BIBO exhibits for a pump wavelength of 800 nm the property that the signal and idler waves travel in opposite directions relative to the pump which ensures exponential growth of the parametric gain even beyond the pulse walk-off length [14]. The higher d_{eff} of BIBO allows, however, the use of thinner crystals to approach shorter (longer) signal (idler) wavelengths for the same gain bandwidth [12]. The effective nonlinearity of BIBO for this type of interaction, assuming a signal wavelength of $\lambda_s=1400\text{ nm}$, is $d_{\text{eff}}=d_{12}\cos\theta=2.38\text{ pm/V}$ [15]. This means that the nonlinear figure of merit [4] of BIBO is roughly two times higher than that of BBO.

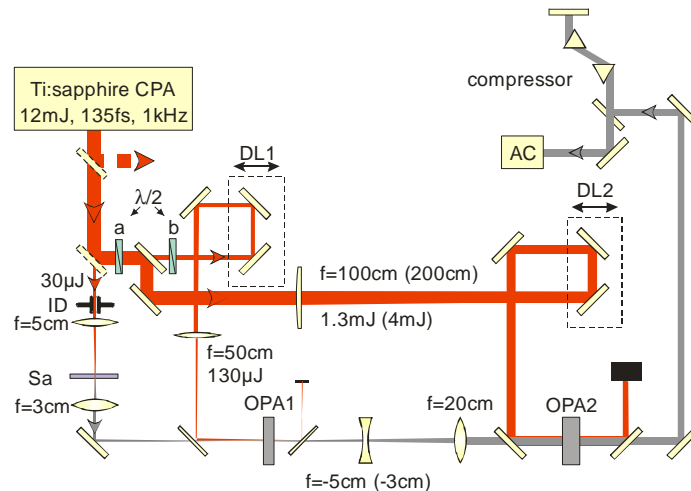


Fig. 1. Schematic of the experimental set-up: CPA, chirped pulse amplifier, OPA1 and OPA2, 1st and 2nd OPA stages, DL, delay lines, ID, iris diaphragm, Sa, sapphire, AC, autocorrelator. The parameters in brackets refer to the high-power version; a and b denote two possible positions of the same half-wave plate ($\lambda/2$).

The second stage could be realized either with type-I or type-II interaction. Type-I $e\rightarrow oo$ interaction in BIBO ensures, however, longer interaction length with the pump pulse and the effective nonlinearity is ≈ 1.3 times higher ($d_{\text{eff}}=d_{12}\cos\theta=3.14\text{ pm/V}$ for $\lambda_s=1400\text{ nm}$). The BIBO crystal available for this purpose was 6-mm thick, uncoated, and had an aperture of $10\times 10\text{ mm}^2$. It was cut at $\theta=11.4^\circ$, also in the x-z principal plane ($\varphi=0^\circ$). Note that, for both stages, d_{eff} of BIBO changes only weakly ($<5\%$) across the entire tuning range, from 1100 to 1600 nm for the signal wavelength.

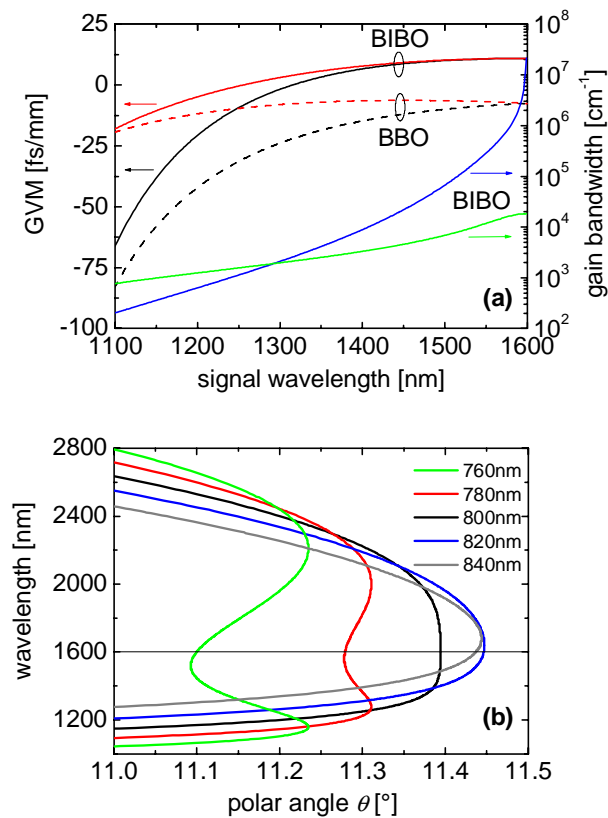


Fig. 2. (a). Inverse group velocity mismatch (GVM) between the pump and idler ($1/v_p - 1/v_i$, black lines) and between the pump and signal ($1/v_p - 1/v_s$, red lines) in type-I, $e \rightarrow \infty$ interaction in BIBO and BBO for a pump wavelength of 800 nm, where v_p , v_s , and v_i denote the pump, signal, and idler group velocities; the blue and green lines show the gain bandwidth (FWHM) for a 6 mm long BIBO type $e \rightarrow \infty$ crystal and a pump intensity of 20 GW/cm², calculated using the first and second order expansion terms in the wave-mismatch, respectively. (b) Phase-matching curves for a BIBO, type $e \rightarrow \infty$ OPA, calculated for several pump wavelengths indicated in the figure.

The main factor which determines the gain bandwidth in optical parametric amplification is the spectral acceptance, defined in the case of a narrow-band wave at the pump wavelength, by the expression $\left| \frac{0.886}{L(v_s^{-1} - v_i^{-1})} \right|$ relating the group velocities of the signal (v_s) and idler (v_i) waves and the crystal length L . As can be easily seen from the difference between the two inverse GVM curves shown in Fig. 2(a), the spectral acceptance is very large for $e \rightarrow \infty$ type BIBO, and larger than that of BBO, not only near degeneracy but also down to $\lambda_s = 1200$ nm. For type-I interaction, the GVM vanishes near degeneracy and second order terms (group velocity dispersion, GVD) have to be taken into account.

From Fig. 2(a) it can also be seen that there is quite a broad spectral range in the case of BIBO only, near $\lambda_s = 1300$ nm, where the signal and idler pulses travel with group velocities very close to that of the pump. This interesting property of BIBO is related to the fact that the present pump wavelength (800 nm) is close to the point where the second harmonic has the same group velocity as the fundamental (1657 nm). In other words this is the point where the dependence of the phase-matching angle for second harmonic generation on the wavelength

has an inflexion point as can be seen from the comparison of the phase-matching curves for $\lambda_p=820$ and 840 nm in Fig. 2(b). It is obvious from Fig. 2(b) that $e \rightarrow \infty$ type BIBO is ideal for broad-band parametric amplification in collinear geometry exactly when the pump wavelength is near 800 nm because the angular dependence of the phase-matching curves is weakest. Retracing behaviour occurs at shorter pump wavelengths.

For calculation of the gain bandwidth [Fig. 2(a)] we took into account the wavelength dependence and the dispersion of refractive indices and computed separately the results obtained with the first (GVM) and the second (GVD) terms assuming, as usually done, a monochromatic pump, plane waves, high gain and no pump depletion [4,14]. The smaller of the two bandwidths should be considered as the correct solution and it is clear that in the $\lambda_s=1100$ - 1300 nm range this is the solution based on the GVM term. Close to degeneracy, however, even the GVD approximation is violated: This is a consequence of the fact that for polarization parallel to the y -axis (o -wave for the present interaction scheme), the GVD vanishes at 1598 nm. Thus, in order to correctly estimate the gain bandwidth when approaching degeneracy, one has to take into account yet higher (third) order terms in the expansion of the wave-mismatch. We will not go here into further details because such procedures critically depend on the accuracy of the Sellmeier equations which have not been refined by phase-matching data, yet [10]. It is important, however, that this exclusive property of BIBO (simultaneous vanishing of both the GVM and GVD terms in collinear interaction) can be used also for generation of broad-band femtosecond continua by pumping near 800 nm, in a similar manner as demonstrated in the past with KDP, pumped at 527 nm in the picosecond regime [16].

The first OPA stage was pumped with an energy of 130 μ J and the position of the type-II BIBO crystal was selected in such a way that it was as close as possible to the focus of the 50 cm pump lens (Fig. 1) but sufficiently far in front of it in order to avoid OPG operation. The output of the first OPA stage (signal plus idler) amounted to several μ J, depending on the wavelength. The second BIBO crystal was placed about 45 cm away from the first stage. Without any additional polarization elements, the second OPA stage could be seeded either only by the amplified signal or only by the generated idler in the first OPA stage. This is a consequence of the fact that different type of interaction is used in the two OPA stages. Initially, we tried seeding of the second OPA stage at the signal wavelength. In this case the half-wave plate (Fig. 1) is in position (a) in order to rotate the pump polarization from horizontal to vertical, i.e. perpendicular to the polarization of the WLC, for both OPA stages.

In the low energy regime of the present experiment, the second OPA stage was pumped by 1.3 mJ and the pump beam was loosely focused by an $f=1$ m lens (Fig. 1). Its shape in the position of the BIBO crystal was slightly elliptical with larger diameter in the horizontal plane. The spot size resulted in a peak axial intensity of ≈ 25 GW/cm². The telescope between the two stages consisted of an $f=5$ cm and an $f=20$ cm lenses (Fig. 1). In this case it was possible to avoid the direct seeding of the second stage by the WLC which occurs at slightly different wavelengths and pump delay (for the second stage) in the whole tuning range by appropriate imaging of the WLC source with the $f=3$ cm collimating lens behind it (Fig. 1). The diameter of the seed beam in the position of the 2nd OPA stage was of the order of 4 - 5 mm. The output energy (signal plus idler) had a maximum of about 350 μ J near $\lambda_s=1200$ nm, it decreased to about 300 μ J at shorter wavelengths ($\lambda_s=1170$ nm) and dropped to 260 μ J close to degeneracy. Thus, the maximum conversion efficiency for this stage was about 27% , or $\approx 34\%$ intrinsic efficiency, taking into account that the crystal is uncoated.

The temporal and spectral characterization was performed by autocorrelation measurements using second harmonic generation in a 0.1 mm thin BBO type-I crystal, and by an $f=15$ cm spectrograph equipped with a 150 l/mm grating blazed for 4 μ m and a 128 -element pyroelectric array as a detector. We also recorded autocorrelation traces after sending the signal pulse through the prism pair (double pass) depicted in Fig. 1. This compressor consisted of two 59° SF11 prisms aligned for minimum deviation (about 80% overall transmission) with vertical off-set for input/output decoupling. This glass material is suitable

only for the signal wavelength and we took care to have minimum glass path, operating just in the vicinity of the apex, by translating the second prism together with the retroreflector relative to the first one. The separation between the prisms was optimised by monitoring third harmonic generation in air or continuum generation in a fused silica plate using an $f=10$ cm focusing lens.

We characterized the low power mode of operation at two signal wavelengths: $\lambda_s=1200$ and 1400 nm. At $\lambda_s=1400$ the wavelength dependence of the gain bandwidth is only weakly pronounced for both stages: The spectral acceptance is narrower for the first stage and broader for the second stage in comparison to operation near $\lambda_s=1200$ nm. Near 1200 nm, the shortest pulses obtained directly from the OPA were 105 fs (FWHM, assuming Gaussian pulse shapes), i.e. roughly 20% shorter than the pump pulses, and their spectral width (26 nm) resulted in a time-bandwidth product of 0.57, very similar to that of the pump pulses.

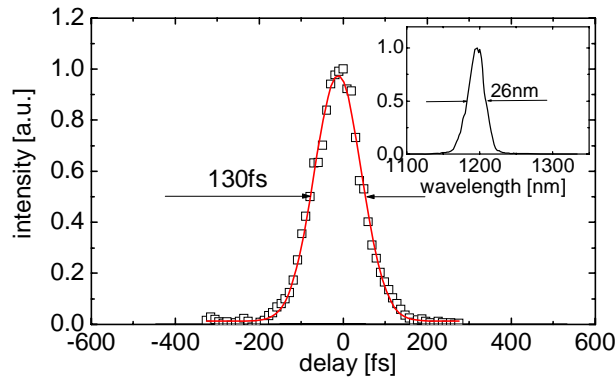


Fig. 3. Autocorrelation trace (symbols) and Gaussian fit (curve) of the compressed signal pulse at 1200 nm from the low-power OPA. The inset shows the corresponding spectrum.

Applying the prism compressor we were able to shorten the signal pulses down to 92 fs which resulted in improvement of the time-bandwidth product down to 0.5. The autocorrelation trace, the Gaussian fit, and the spectrum are shown in Fig. 3. The performance of the OPA at $\lambda_s=1400$ nm was very similar. In general, the optimum prism separation critically depended on the alignment of the OPA. Hence, having in mind the modest compression factors achieved, we did not implement the compressor in the high power regime.

In order to study the energy scaling potential of the present OPA the pump energy for the second stage was increased to 4 mJ. Exchanging the beam splitters, it was possible to preserve the same pumping conditions for the WLC generation and the first OPA stage. The focal length of the lens used for pumping the second stage was increased to 200 cm; the distance from this lens to the second OPA stage was about 100 cm. Simultaneously, the negative lens of the telescope used for expansion of the seed beam from the first OPA stage (Fig. 1) was substituted by another one with $f=-3$ cm in order to better match the pump beam cross section in the position of the second OPA stage. The pump beam completely filled the aperture of the BIBO crystal used in the 2nd OPA stage. Its spatial distribution was somewhat elliptical but very close to Gaussian: Fitting gave a FWHM (intensity) of 10.1 mm in the horizontal and 6.5 mm in the vertical direction. This results in a peak on-axis intensity of ≈ 40 GW/cm², which corresponds to the 20 GW/cm² assumed in Fig. 2(a) in the plane wave approximation.

Seeding still with the signal pulse from the first OPA stage, the maximum energy obtained from the second OPA stage reached 1.1 mJ (signal plus idler) near $\lambda_s=1200$ nm. The output was also somewhat elliptical with horizontal and vertical beam diameters of ≈ 7 and ≈ 4.5 mm, respectively. The signal spectra recorded had a short-wave shoulder and the autocorrelation

traces indicated the presence of satellite pulses and/or a longer pedestal. This was a consequence of simultaneous direct seeding of the second OPA stage by the WLC, at the same position of the delay lines. This effect was absent only in the limit of the tuning range, for signal wavelengths approaching 1100 nm. Figure 4 shows the recorded signal spectrum (inset) and the corresponding autocorrelation function at $\lambda_s=1120$ nm, where the total output energy (signal plus idler) amounted to 1 mJ, corresponding to an intrinsic conversion efficiency of $\approx 32\%$ for the second stage. The deconvolved pulse duration assuming Gaussian pulse shape was ≈ 140 fs (FWHM) which gives a time-bandwidth product of 0.85.

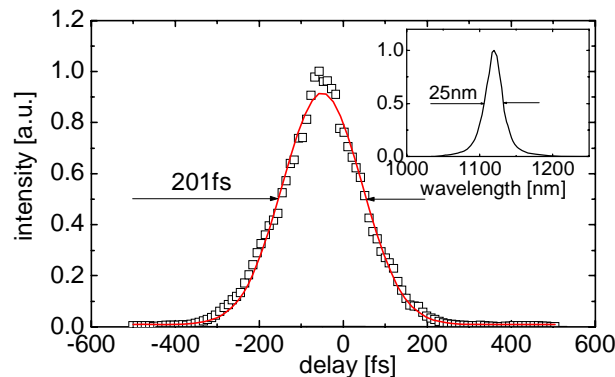


Fig. 4. Autocorrelation trace (symbols) and Gaussian fit (curve) of the signal pulse at 1120 nm from the high-power OPA with seeding at the signal wave. The inset shows the corresponding spectrum.

At longer signal wavelengths the contribution of the direct seed from the WLC stage continuously increased and near 1300 nm became the main factor that determined the output energy from the second OPA stage. In the high-power regime it was not possible to eliminate this effect related to the broad gain bandwidth of the second stage by modifying the imaging of the WLC and the seed from the first stage. The restrictions are related also to the fact that the second OPA stage is operated at quite high gain. One possibility to avoid this is the introduction of an intermediate OPA stage, however, this would greatly increase the complexity. The second possibility, which is more elegant, is to seed the second OPA stage only by the idler generated in the first OPA stage. This was realized by simply shifting the half-wave plate to position (b) in Fig. 1, and rotation of the $e \rightarrow \infty$ BIBO crystal by 90° . Thus, the WLC has the same extraordinary polarization (in the horizontal plane) as the pump for the second OPA stage and no phase-matching is possible.

In general, seeding at the idler wavelength produced energy output which was roughly 80% of the total output when seeding at the signal wavelength was applied. Thus, near $\lambda_s=1200$ nm, the total output energy seeding with the idler from the 1st OPA stage amounted to 850 μ J. Towards degeneracy the energy dropped to roughly 600 μ J. The spectra measured at two signal-idler pairs are shown in Fig. 5. In Fig. 6 the corresponding autocorrelation traces with their FWHM are presented. The latter were well fitted by Gaussian curves. The resulting pulse durations were almost constant, varying only from 133 to 139 fs, i.e. very close to the pump pulse duration. The time-bandwidth products near degeneracy (see Fig. 6) were also very close to the product for the pump pulses, away from degeneracy they were slightly larger. The values correspond to roughly 1.5-2 times the Fourier limit for Gaussian pulses.

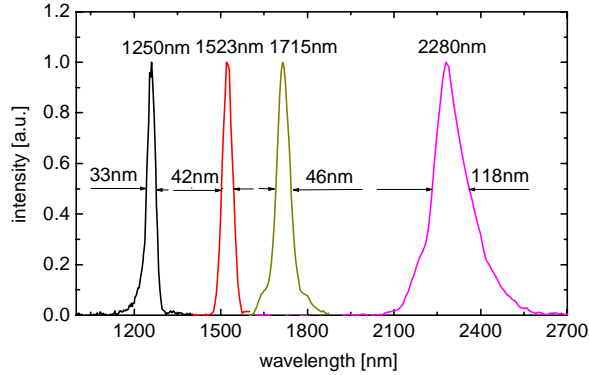


Fig. 5. Spectra of the high-power OPA with idler seeding, recorded for two signal-idler pairs at a total output energy of 600 μJ (near degeneracy) and 800 μJ (away from degeneracy).

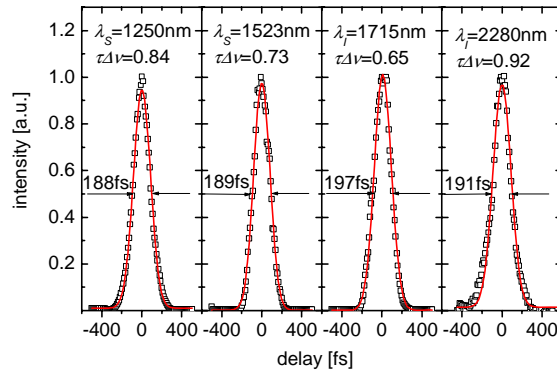


Fig. 6. Autocorrelation traces (symbols) and Gaussian fits (curves) with FWHM for the signal and idler pulses corresponding to the spectra from Fig. 5. The time-bandwidth products are also given in the figure.

In conclusion, using BIBO crystals in a two stage near-IR femtosecond OPA we were able to increase the output energy roughly 5 times in comparison to previous work with BBO at 1 kHz repetition rate. The maximum energy obtained for a signal wavelength of 1200 nm was 1.1 mJ (signal plus idler) and the tunability extended from 1.1 to 2.9 μm . Further improvement of the present results in terms of energy scaling can be expected by using antireflection coated crystals of yet larger aperture (larger than 1 cm^2). This would allow full utilization of the currently available pump energies from specially designed high-power Ti:sapphire amplifier systems. Output energies from the OPA as high as 2 mJ seem realistic, however, optimization of such systems might require the addition of a further (third) amplification stage. The monoclinic crystal BIBO possesses very suitable and unique properties for broadband parametric amplification when pumped near 800 nm in collinear geometry. Hence, it is a very promising candidate for a wide range of femtosecond down-conversion schemes based on Ti:sapphire laser pump sources.

Acknowledgments

We acknowledge financial support from the German-Bulgarian exchange programme (DAAD grant D/05/11319 and Bulgarian Ministry of Science and Education grant D01-81/2006), and from the Laserlab Europe (contract RII3-CT-2003-506350). M. Ebrahim-Zadeh gratefully acknowledges personal support of the Institucio Catalana de Recerca i Estudis Avancats (ICREA), Passeig Lluís Companys 23, Barcelona 08010, Spain.